

# Grazing incidence x-ray fluorescence and secondary ion mass spectrometry combined approach for the characterization of ultrashallow arsenic distribution in silicon

G. Peponi,<sup>a)</sup> D. Giubertoni, and M. Bersani

*CMM-Irst, Fondazione Bruno Kessler, via Sommarive 18, 38123 Povo, Trento, Italy*

F. Meirer,<sup>b)</sup> D. Ingerle, G. Steinhauser, and C. Strelt

*Atominstytut, Technische Universität Wien, Stadionallee 2, 1020 Wien, Austria*

P. Hoenicke and B. Beckhoff

*Physikalisch-Technische Bundesanstalt, Abbestr. 2-12, 10587 Berlin, Germany*

(Received 22 June 2009; accepted 21 December 2009; published 1 March 2010)

Dopant depth profiling and dose determination are essential for ultrashallow junction technology development. However they pose a challenge to the widely used dynamic secondary ion mass spectroscopy (SIMS) technique that suffers uncertainties due to an initial transient width comparable to the dopant depth distribution. In this work the authors report on the application of grazing incidence x-ray fluorescence (GIXRF) for arsenic in silicon dose and profile determination and its combination with SIMS in order to try to overcome the limitations of the latter in the topmost few nanometers. A polynomial variation of the sputtering rate is supposed in the first sputtering stage of the SIMS analysis and the parameters that regulate the magnitude of such correction are determined by a least square fitting of the angle dependent fluorescence signal. The total retained fluence was also measured by instrumental neutron activation analysis and synchrotron radiation soft x-ray GIXRF. The comparison among the total retained fluence determinations shows a good agreement among the techniques. Furthermore, from this first set of measurements it was clearly shown that the GIXRF profile correction is very sensitive to the SIMS profile in the very first nanometers. Therefore if matrix effects are present in the SIMS analysis beside the sputtering rate change, the tested sputtering rate correction can produce nonreliable profiles. © 2010 American Vacuum Society. [DOI: 10.1116/1.3292647]

## I. INTRODUCTION

The introduction of ultrashallow junctions for source and drain extensions of Si complementary metal oxide semiconductor devices has represented a challenge for well established depth profiling analytical techniques, such as secondary ion mass spectrometry (SIMS).<sup>1</sup> In fact, the latter is still able to evaluate the junction depth in implanted blanket wafers given the excellent detection limits ( $\sim 1 \times 10^{16} \text{ cm}^{-3}$ ) and the depth resolution adequate for probing the abruptness of most distributions as long as the impact energy of the primary ion beam is scaled down. However, two main drawbacks are apparently unsolvable: first, the impossibility of reaching the combination of lateral resolution and detection limit necessary for two- and three-dimensional characterizations;<sup>2</sup> second, the unavoidable initial transient width,<sup>3</sup> i.e., the depth to be sputtered before equilibrium between implanted and resputtered primary ions is established. This effect is particularly relevant when reactive ions such as  $\text{O}_2^+$  or  $\text{Cs}^+$  are used to enhance ion yield and thus the sensitivity. In fact, strong variations of sputtering and ion yield are often observed in this transient width and an accurate calibration of both depth and concentration scale is not trivial.<sup>4</sup>

Furthermore, early formation of roughness has been reported for sputtering Si with ultralow energy (ULE) ions at oblique incidence<sup>5,6</sup> with further consequent variation of sputtering and ion yield. As an obvious consequence the dose evaluation of ultrashallow junctions is difficult to obtain by SIMS because a significantly large fraction of dopant is confined in this initial transient depth. As far as  $\text{Cs}^+$  sputtering is concerned, an analytical approach often applied for *n*-type dopant depth profiling in Si, Parisini *et al.*<sup>7</sup> recently showed that SIMS determined profiles are not correct as they are too close to the surface, confirming earlier findings. Much work has been done in the past trying to take into account sputtering rate (SR) and/or sensitivity factor changes in the initial phase.<sup>8-11</sup> For instance, van der Heide *et al.*<sup>8</sup> investigated the SR changes due to the early formation of roughness when sputtering Si with ULE  $\text{Cs}^+$  beam at oblique incidence. Investigating a B delta doped Si sample, they proposed a polynomial relation for the relative sputtering rate variations, i.e., the ratio between the actual SR and the one obtained from the measurement of the final crater depth,

$$\text{SR}_{(\text{rel})} = (1/(0.06\text{AD}^2 - 0.01\text{AD} + C)) + 0.99, \quad (1)$$

where AD is the apparent depth obtained converting the sputtering time to depth using the final crater depth and *C* was a factor determined by fitting.<sup>10,11</sup>

<sup>a)</sup>Electronic mail: peponi@fbk.eu

<sup>b)</sup>Present address: Stanford Synchrotron Radiation Lightsource, 2575 Sand Hill Road, Menlo Park.

Since the dopant atoms in ultrashallow junctions are mostly confined to the first few nanometers, alternative techniques such as angle-resolved x-ray photoelectron spectroscopy<sup>12</sup> and grazing incidence x-ray fluorescence (GIXRF), whose probing depths are around 10 nm, can be applied to evaluate the retained dose and possibly the depth distribution of the dopant.<sup>13</sup> In particular, in GIXRF the sampling depth can be varied by changing the x-ray beam incidence angle from zero up to a couple of times the critical angle for total reflection. In this way, the variation of the fluorescence signal as a function of the incidence angle gives indications on the depth distribution of the excited species. Such information though is convoluted with the x-ray standing wave field intensity as expressed by the following relationship:

$$I_{\text{fluorescence}} \propto \int c(z)f(z)dz, \quad (2)$$

where  $f(z)$  includes all phenomena linked to the depth dependence of the fluorescence radiation (field intensity, absorption of incoming, and outgoing radiation). Hence the profile concentration is not readily obtainable with the measurement.<sup>14,15</sup> In the case of As ultrashallow distributions in Si, Pepponi *et al.*<sup>13</sup> compared the experimental grazing incidence fluorescence signals and the simulated ones with input concentration profiles obtained by SIMS with different quantification procedures in order to evaluate the SIMS accuracy. In this work, such an approach is extended by implementing a depth scale correction as the aforementioned one proposed by van der Heide: The simulation of the GIXRF As signal is combined with a fitting procedure where the SIMS profile is modified only on the depth scale according to Eq. (1) where  $C$  is the fitting factor. In Fig. 1 a flow chart depicts the algorithm. This correction model was originally developed mostly to take into account changes in the sputtering rate due to roughening of the crater bottom, but allowed also smaller corrections where no roughening was visible. Moreover, since the total retained dose is proportional to the overall fluorescence intensity and independent of the profile shape, a procedure for dose evaluation was developed.

The reason for the combined approach is that there are several artifacts in the near surface of a SIMS profile. The depth over which these artifacts affect SIMS profiles varies and depends on the net primary beam energy, incident angle, bombarding species, and matrix. For ultrashallow implants a substantial portion of the dopant could be in the region affected by these SIMS artifacts. However, the dopant concentrations are sufficiently high and close enough to the surface that GIXRF analysis is completely feasible. This suggests that a combined approach could lead to a more accurate determination of dose and projected range.

Besides SIMS and GIXRF two additional, independent methods for dose determination were carried out for comparison: soft x-ray synchrotron radiation GIXRF and instrumental nuclear activation analysis.

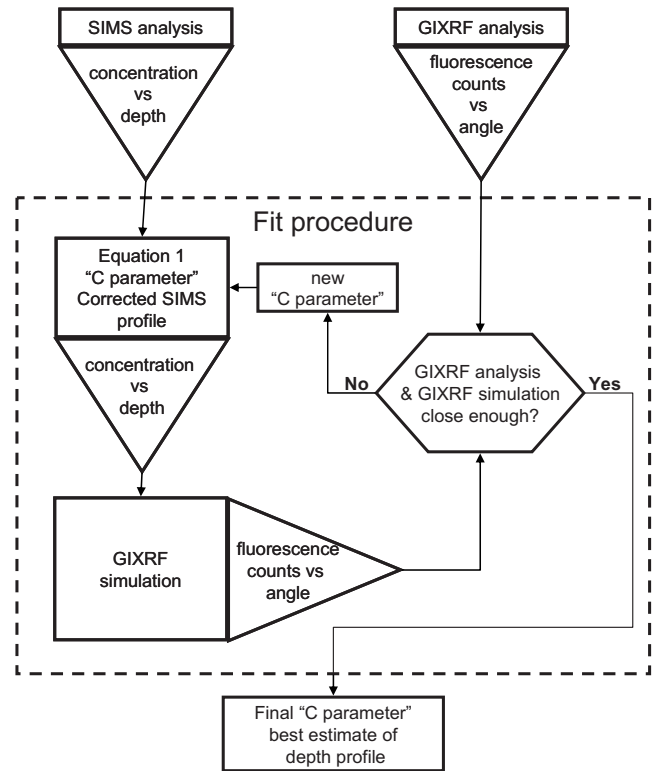


FIG. 1. Flow chart depicting the algorithm implemented for fitting the GIXRF experimental data by correction the SIMS profile given as initial best estimate.

## II. EXPERIMENT

<sup>75</sup>As<sup>+</sup> was implanted in the Czochralski (100) Si wafers (300 mm in diameter) at 0° tilt and twist angles with an Applied Materials Quantum X implanter to produce two sets of samples: one with a constant nominal fluence of  $1 \times 10^{15}$  atoms/cm<sup>2</sup> and implantation energies of 0.5, 1, 2, 3, and 5 keV and one with a constant implantation energy of 2 keV and varying nominal fluence of  $1 \times 10^{14}$ ,  $5 \times 10^{14}$ ,  $1 \times 10^{15}$ , and  $5 \times 10^{15}$  atoms/cm<sup>2</sup>. The samples were then analyzed with a CAMECA Wf/SC-Ultra, magnetic sector secondary ion mass spectrometer, with a Cs<sup>+</sup> sputtering beam with impact energies of 0.25 keV (~40° incidence), 0.35 keV (~45°), and 0.50 keV (~45°), respectively. <sup>28</sup>Si <sup>75</sup>As<sup>-</sup> and <sup>28</sup>Si<sub>2</sub><sup>-</sup> negative secondary ions were collected from a 66 μm diameter area centered in a 250 × 250 μm<sup>2</sup> crater in high mass resolution ( $M/\Delta M \sim 2500$ ). Sputtering time was converted to depth using a single constant SR as determined from the measurement of the final crater depth. <sup>28</sup>Si <sup>75</sup>As<sup>-</sup> secondary ion intensity was converted to As concentration using a relative sensitivity factor (RSF) determined from an As implant in Si ( $1.25 \times 10^{14}$  cm<sup>-2</sup>/5 keV) of known dose. The RSF was measured at the beginning and at the end of each analysis run normalizing to the average of the <sup>28</sup>Si<sub>2</sub><sup>-</sup> signal after the steady sputtering equilibrium had been achieved. No corrections were applied to the RSF in the initial transient width, surface SiO<sub>2</sub> layer, and its interface with Si substrate.<sup>16</sup>

Grazing incidence x-ray fluorescence measurements have been carried out with an instrument developed at the Atominstitut of the Vienna University of Technology. The instrument consists of an aluminum vacuum chamber (typical pressure 1 mbar) inside, which an XYZ $\omega$  stage is mounted for sample positioning (at  $\omega=0$  the sample is horizontal). A diffraction x-ray tube housing is mounted vertically onto one sidewall of the chamber and connected to the chamber through a polyimide window. A radiant vortex silicon drift detector with an active area of 50 mm<sup>2</sup> is used for the detection of the fluorescence. The cold finger of the detector enters the chamber from the top. The detector window (8  $\mu$ m thick Be) is positioned about 2 mm above the sample surface. Self-developed software allows the control of the motors and reading of the x-ray spectrum from the detector electronic and automated scans can be programmed. Si  $K\alpha$  and As  $K\alpha$  photon intensities were extracted from the spectrum by integration of the counts in the relative regions of interest, basic trapezoidal background removal, and dividing through the spectrum acquisition live time.

Simulation of the fluorescence signal of the substrate and of the dopant according to a given concentration profile was carried out as described in Ref. 13. The simulation assumes that the dopant does not change the optical properties of the substrate. A least-squares fitting procedure on the substrate signal (in this case Si  $K\alpha$ ) is used to determine the angular offset (in the apparatus the angular step is mechanically determined whereas the absolute angle of the sample with respect to the beam can be slightly different after each sample change), the beam divergence, and a scaling factor  $k_{\text{substrate}}$  taking into account instrumental parameters and including the sensitivity for the substrate element. A second fitting procedure on the dopant signal is used to determine the  $C$  factor contained in Eq. (1) (and therefore the corrected depth of the input profile) and a scaling factor  $k_{\text{dopant}}$  for the dopant. The  $C$  factor corrects the depth calibration and thus the determined projected range of As implants, whereas the scaling factor is directly linked to the total retained fluence. After the application of Eq. (1) the depth profile is normalized to keep the total dose constant. The ratio between the scaling factors (substrate and dopant) only depends on the elements and transitions chosen for the analysis and, in particular, it is independent from the primary beam intensity on the sample. It must be mentioned that if measurements are carried out in a medium presenting different absorptions of the fluorescence radiation for the substrate and the dopant, the ratio among scaling factors will be dependent of the distance between sample and detector. The total retained dose is then determined by comparison with a sample with known dose according to the relation

$$\frac{k_{\text{substrate,std}}}{k_{\text{dopant,std}}} \text{total dose}_{\text{std}} = \frac{k_{\text{substrate,unknown}}}{k_{\text{dopant,unknown}}} \text{total dose}_{\text{unknown}}, \quad (3)$$

where  $\text{total dose}_{\text{std}}$  is the known total retained fluence of a reference sample,  $k_{\text{substrate,std}}$  and  $k_{\text{dopant,std}}$  are the scaling factors determined experimentally for the known reference

sample, and  $k_{\text{substrate,unknown}}$  and  $k_{\text{dopant,unknown}}$  are the scaling factors determined experimentally for the unknown.

Simulations show that the high angle (well above the critical angle) fluorescence signal is independent from the profile shape but only depends on the total retained dose (this is not rigorously true, but for very shallow profiles the differences are well below the measurement error). Quantification was carried out using the same standard sample used for SIMS.

Instrumental neutron activation analysis (INAA) measurements were carried out at the TRIGA Mark II reactor of the Atominstitut, Vienna University of Technology, as previously reported.<sup>17</sup> Samples were irradiated for 1200 s using the pneumatic sample transfer system (neutron flux density of  $\sim 3 \times 10^{12}$  cm<sup>-2</sup> s<sup>-1</sup>). After a cooling time of at least 60 min, the <sup>76</sup>As ( $T_{1/2}=1.0942d$ ; 559 keV) activities were determined with a 222 cm<sup>3</sup> HPGe semiconductor detector. The measurement times were chosen independently for each sample, until the error due to counting statistics was <5% relative to the <sup>76</sup>As peak in each spectrum. The total number of As atoms in the piece of wafer analyzed was determined by assuming that the sample with higher dose contained exactly  $5 \times 10^{15}$  atoms/cm<sup>2</sup>.

The SR-GIXRF measurements were performed with irradiation chamber of the Physikalisch-Technische Bundesanstalt for 200 and 300 mm silicon wafers by employing monochromatized undulator radiation at the plane grating monochromator beamline for undulator radiation at BESSY II.<sup>18</sup> This beamline provides monochromatized undulator radiation in the energy range from 78 up to 1860 eV. The beam, partially reflected on the wafer surface, is associated with a standing wave field, which is dependent on both the incident photon energy and the angle of incidence. The strong modulations of the intensity of the incident radiation at the wafer surface, caused by a changing standing wave field, result in an angle and depth dependent intensity distribution inside the doped silicon. The implantation depth profile is convolved with this intensity distribution, which has been calculated with the IMD software package<sup>19</sup> and creates a specific fluorescence curve when a GIXRF measurement is performed. Since all parameters involved except for the depth distribution of the implant are known, the GIXRF curve can be calculated using an appropriate assumption on the form of the profile. By comparison of calculated and measured curve one may confirm this assumed depth distribution. For the analysis of the samples, a completely reference-free, fundamental parameter based method was employed.<sup>20</sup> Here, the incident photon flux is recorded by absolutely calibrated photodiodes and the solid angle of detection (of the fluorescence radiation) is defined by means of a calibrated diaphragm. For the detection of the fluorescence radiation itself, detectors with both well-known spectral efficiency and response behavior were used. Based on this instrumentation, the absolute dose value can then be calculated by numerical integration of the confirmed depth profile without the need for any further reference sample or external normalization standards.

TABLE I. Total retained fluence obtained with SIMS at impact energies of 0.25, 0.35, and 0.5 keV.

Sample id	Implant energy (keV)	Total retained fluence (atoms/cm <sup>2</sup> )			
		Nominal	SIMS 500 eV	SIMS 350 eV	SIMS 250 eV
As1	0.5	$1.0 \times 10^{15}$	$1.1 \times 10^{15}$	$1.0 \times 10^{15}$	$9.8 \times 10^{14}$
As2	1	$1.0 \times 10^{15}$	$1.1 \times 10^{15}$	$1.1 \times 10^{15}$	$1.0 \times 10^{15}$
As3	2	$1.0 \times 10^{15}$	$1.0 \times 10^{15}$	$1.1 \times 10^{15}$	$1.1 \times 10^{15}$
As4	3	$1.0 \times 10^{15}$	$1.1 \times 10^{15}$	$1.1 \times 10^{15}$	$1.1 \times 10^{15}$
As5	5	$1.0 \times 10^{15}$	$1.1 \times 10^{15}$	$1.1 \times 10^{15}$	$1.1 \times 10^{15}$
As6	2	$1.0 \times 10^{14}$	$1.1 \times 10^{14}$	$1.0 \times 10^{14}$	$1.0 \times 10^{14}$
As7	2	$5.0 \times 10^{14}$	$5.5 \times 10^{14}$	$5.5 \times 10^{14}$	$5.5 \times 10^{14}$
As8	2	$5.0 \times 10^{15}$	$4.6 \times 10^{15}$	$4.5 \times 10^{15}$	...

### III. RESULTS AND DISCUSSION

The total retained fluence for all samples obtained with SIMS at the three impact energies is reported in Table I. The overall uncertainty of the SIMS dose determination is about 7%–8%. The uncertainty on the sputtering rate (that as mentioned above affects the evaluation of the total retained fluence) was calculated taking into account the uncertainty in the crater depth (evaluated from three to five measurements per crater) and primary beam intensity fluctuations.

SIMS measurements of the  $1 \times 10^{15}$  atoms/cm<sup>2</sup> implants at various energies produce dose values that are the same within error suggesting reduced matrix effects in those experimental conditions.

The dose values measured by SIMS (500 eV) are compared to the results obtained with GIXRF, SR-GIXRF, and INAA in Figs. 2 and 3. GIXRF repeatability was estimated on another sample (Si:As  $7.99 \times 10^{14}$  cm<sup>-2</sup>/5 keV) which was measured six times: five measurements have been quantified keeping one as standard; the relative standard deviation of these quantifications was 3.4% and this was adopted as uncertainty for the GIXRF measurements. This is probably underestimated for the lower dose samples. The uncertainty of the INAA measurements is mainly due to the counting statistics, and as mentioned above this should be within 5%. For SR-GIXRF an uncertainty of 10% was estimated. Good

agreement (within a 10%) is observed among the different techniques and in accordance with the estimated uncertainties. No general trend or systematic error is evident. For all analyzed samples, simulations of the implantation profile have been calculated using the software SRIM (version 2008.04) accounting for the full damage cascades.

Figure 4 reports the experimental GIXRF data (fluorescence intensity versus x-ray incidence angle) with the simulated curves for the SIMS 500 eV profile and the SRIM profile as well as those profiles changed by the fitting procedure. The profiles determined with SIMS at the three impact energies as well as a SRIM simulation of the implant and the profiles changed by the GIXRF depth scale correction for sample As1 are shown in Fig. 5.

In Figs. 6 and 7 projected range and straggle of the 0.5 keV impact energy SIMS measurements and values obtained after fitting of the GIXRF data are represented. The projected range values are displayed as the data point whereas the straggle ones have been shown as symmetrical error bars.

For all samples the projected range is moved into the depth as often observed<sup>21</sup> but by an extent larger than expected. In fact, the resulting As distributions have an Rp even deeper than the one expected from SRIM whereas past results from different techniques, e.g., medium energy ion scattering,<sup>22</sup> revealed that usually the opposite holds, i.e.,

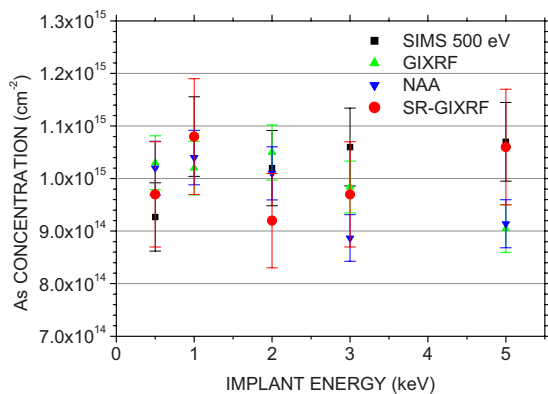


FIG. 2. (Color online) Total retained fluence obtained with SIMS at 0.50 keV impact energy, GIXRF, SR-GIXRF, and INAA for the samples with constant nominal fluence of  $1 \times 10^{15}$  cm<sup>-2</sup>.

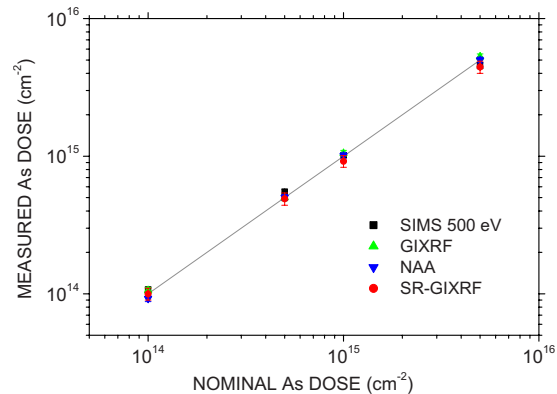


FIG. 3. (Color online) Total retained fluence obtained with SIMS at 0.50 keV impact energy, GIXRF, SR-GIXRF, and INAA for the samples with constant implantation energy of 2 keV are displayed.

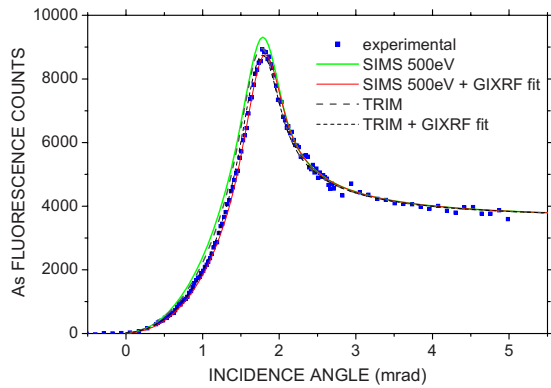


FIG. 4. (Color online) GIXRF experimental data and simulation of the fluorescence curve with the 0.5 keV impact energy SIMS profile, the SRIM profile, and those profiles changed by the GIXRF data fitting procedure.

SRIM is deeper than the actual peak position. Furthermore, the decay length of the GIXRF corrected curve is dramatically increased. Those findings seem to suggest that the depth calibration correction alone introduces inaccuracies in the obtained As profiles and thus a more sophisticated model has to be developed considering also a concentration calibration correction in the top nanometers. However, some trends are evident and can give useful indications. The corrected Rp values present an increasing shift (with respect to SIMS) for samples implanted with energy from 0.5 to 3 keV and decreasing for the two higher implantation energies. This is consistent with a higher sensitivity of GIXRF to dopant distribution variations in the very near surface region, whereas when most dopant is confined in the bulk, the angular scan is poorly affecting the fluorescence signal and thus smaller corrections are expected.

The GIXRF fits related to the implants with higher fluences ( $1 \times 10^{15}$  and  $5 \times 10^{15}$ ) show a larger increase in the corrected projected range than the lower dose implants ( $1 \times 10^{14}$  and  $5 \times 10^{14}$ ). This may suggest that the higher the dose, the higher is the overestimation of As in the first nanometers, an effect which apparently cannot be taken into account only with the correction of the sputtering rate.

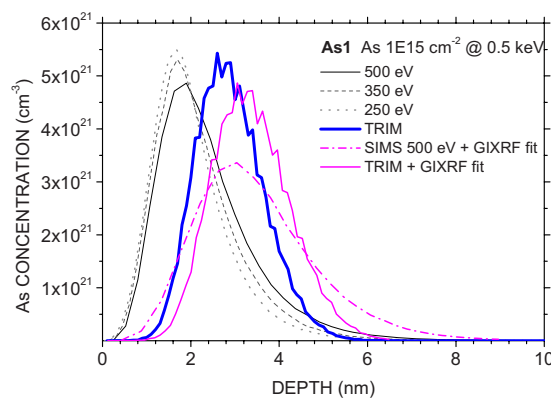


FIG. 5. (Color online) SIMS profiles at the different energies, SRIM simulated profile; SIMS profiles with impact energy of 0.5 keV and SRIM profiles as modified by the GIXRF fitting procedure.

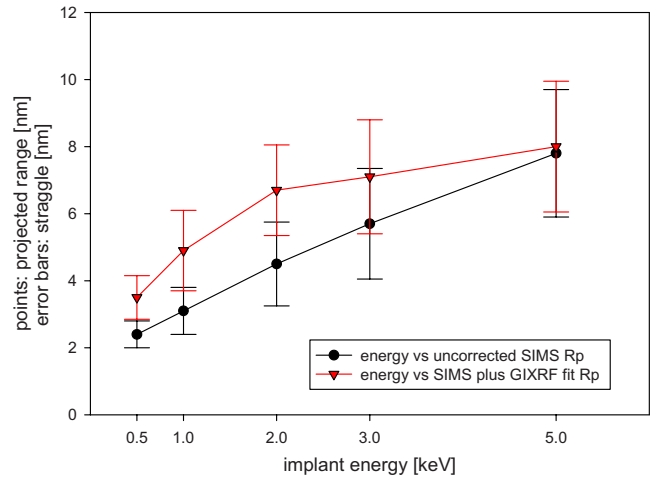


FIG. 6. (Color online) Projected range (data points) and straggle (error bars) of original SIMS (impact energy 0.5 keV) measurement and after the sputtering rate corrections obtained by GIXRF data fitting vs implant energy for samples with constant nominal fluence of  $1 \times 10^{15}$  cm<sup>-2</sup>.

#### IV. CONCLUSIONS

The total retained fluence of eight ultralow energy As implants has been determined with SIMS and laboratory based GIXRF and checked with independent methods, such as INAA and SR-GIXRF. The values are generally in agreement with estimated uncertainties of 5%–10%. SIMS measurements obtained with different primary beam sub-keV impact energies show no relevant differences in the total retained dose determination.

The SIMS sputter rate decreases with depth in the early stages of an analysis, so if an average sputter rate is used, Rps are apparently shifted toward the surface in the resulting depth profile. This analysis artifact is not present for GIXRF and the combined approach did shift the peaks in the expected direction. However the basic approach taking into account only changes in sputtering rate does not seem to con-

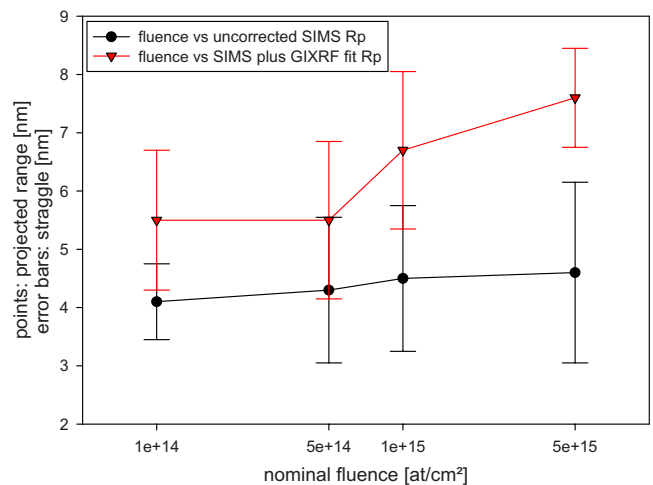


FIG. 7. (Color online) Projected range (data points) and straggle (error bars) of original SIMS (impact energy 0.5 keV) measurement and after the sputtering rate corrections obtained by GIXRF data fitting vs dose for the 2 keV implants.

sistently provide reliably corrected profiles. The inclusion of ion yield changes due to matrix effects in early stages of the SIMS analysis would probably provide much better results but further work is needed in order to supplement the fitting procedures with such corrections.

## ACKNOWLEDGMENTS

The authors would like to thank Majeed Foad and Tze Poon of FEP, Applied Materials, Santa Clara, for providing the samples. The presented work was carried out within the framework of the project ANNA, an Integrated Infrastructure Initiative financed under Framework Program 6 by the European Commission (Project No. 026134).

<sup>1</sup>W. Vandervorst *et al.*, *Appl. Surf. Sci.* **231–232**, 618 (2004).

<sup>2</sup>W. Vandervorst, *AIP Conf. Proc.* **931**, 233 (2007).

<sup>3</sup>K. Wittmaack, *Appl. Surf. Sci.* **203–204**, 20 (2003).

<sup>4</sup>W. Vandervorst, T. Janssens, R. Loo, M. Caymax, I. Peytier, R. Lindsay, J. Fruhauf, A. Bergmaier, and G. Dollinger, *Appl. Surf. Sci.* **203–204**, 317 (2003).

<sup>5</sup>Z. X. Jiang and P. F. A. Alkemade, *J. Vac. Sci. Technol. B* **16**, 1971 (1998).

<sup>6</sup>Y. Kataoka, K. Yamazaki, M. Shigeno, Y. Tada, and K. Wittmaack, *Appl. Surf. Sci.* **203–204**, 43 (2003).

<sup>7</sup>A. Parisini, V. Morandi, S. Solmi, P. G. Merli, D. Giubertoni, M. Bersani, and J. A. Van den Berg, *Appl. Phys. Lett.* **92**, 261907 (2008).

<sup>8</sup>P. A. W. van der Heide, M. S. Lim, S. S. Perry, and J. Bennett, *Nucl. Instrum. Methods Phys. Res. B* **201**, 413 (2003).

<sup>9</sup>P. A. W. van der Heide, *Appl. Surf. Sci.* **252**, 6456 (2006).

<sup>10</sup>T. Janssens and W. Vandervorst, in *Proceedings of the 12th Secondary Ion Mass Spectrometry International Conference*, edited by P. Bertrand, H.-N. Migeon, and H. W. Werner (Elsevier, New York, 2000), p. 401.

<sup>11</sup>K. Wittmaack, *Surf. Interface Anal.* **26**, 290 (1998).

<sup>12</sup>G. Saheli, G. Conti, Y. Uritsky, M. A. Foad, C. R. Brundle, P. Mack, D. Kouzminov, M. Werner, and J. A. van den Berg, *J. Vac. Sci. Technol. B* **26**, 298 (2008).

<sup>13</sup>G. Pepponi, C. Strelti, P. Wobrauschek, N. Zoeger, K. Luening, P. Pianetta, D. Giubertoni, M. Barozzi, and M. Bersani, *Spectrochim. Acta, Part B* **59**, 1243 (2004).

<sup>14</sup>C. Steen *et al.*, *J. Appl. Phys.* **104**, 023518 (2008).

<sup>15</sup>L. Pei *et al.*, *J. Appl. Phys.* **104**, 043507 (2008).

<sup>16</sup>D. Giubertoni, M. Bersani, M. Barozzi, S. Pederzoli, E. Iacob, J. A. van den Berg, and M. Werner, *Appl. Surf. Sci.* **252**, 7214 (2006).

<sup>17</sup>G. Steinhauser, J. H. Sterba, M. Bichler, and H. Huber, *Appl. Geochem.* **21**, 1362 (2006).

<sup>18</sup>B. Beckhoff, R. Fliegau, M. Kolbe, M. Müller, J. Weser, and G. Ulm, *Anal. Chem.* **79**, 7873 (2007).

<sup>19</sup>D. Windt, *Comput. Phys.* **12**, 360 (1998).

<sup>20</sup>B. Beckhoff, *J. Anal. At. Spectrom.* **23**, 845 (2008).

<sup>21</sup>Y. Kataoka and T. Itani, *Surf. Interface Anal.* **39**, 826 (2007).

<sup>22</sup>J. A. van den Berg *et al.*, *Proceedings of the 14th International Conference on Ion Implantation Technology, 2002* (unpublished), pp. 597–600.